

The impact of the cut-out shape on the dynamic behavior of composite thin circular plates

Oguzhan Das

Department of Motor Vehicles and Transportation Technologies, Dokuz Eylül University, Izmir, Turkey.

Corresponding Author: oguzhan.das@deu.edu.tr

Submitted : 22/09/2021

Revised : 06/01/2022

Accepted : 19/01/2022

ABSTRACT

This study measures the impact of the cut-out shape on the fundamental frequency and the harmonic response of thin composite circular plates under fixed boundary conditions. For this purpose, the Finite Element Method has been employed using the SHELL181 element of ANSYS Workbench 18.2 software. Nine different circular plates having central equilateral triangle, square, regular pentagon, regular hexagon, regular heptagon, regular octagon, regular nonagon, regular decagon, and circular cut-outs have been designed to understand the changes in the vibrational behavior of a structure as the cut-out geometry approximates to circular. Additionally, a solid circular plate has been modelled for comparison purposes. To investigate the effect of the cut-out shape more deeply, all structures have been designed as cross-ply and angle-ply composites. The free vibration analysis has been performed to obtain the fundamental frequency of each structure. The harmonic response analysis problem has been solved by employing the Mode Superposition Method and considering a constant damping ratio. The results of the study have been interpreted by considering the displacement response, stress, and phase shifts at a certain frequency range. The results indicate that the shape of the cut-out considerably affects the fundamental frequency and harmonic response of the circular structure regardless of its fiber orientation.

Keywords: Harmonic response; Circular plates; Cut-out shape; Finite element analysis.

INTRODUCTION

Circular plates with cut-outs have been employed in various engineering fields. The vibration behavior of these structures has been investigated by many researchers since they may be subjected to loads that may lead these structures to fail due to the phenomenon called resonance. Besides, such loads may also cause damage in these structures due to the excessive vibration that may cause high stress and displacement. Although there are various studies covering the vibrational behavior of structures (Sivandi-Pour et al., 2020, Çelebi et al., 2018, Albassam, 2021, Javed et al., 2018, & Gonenli & Das, 2021) including harmonic response analysis (Yu et al., 2017, Jiaqiang et al., 2019, Kumar & Sarangi, Liu et al., 2021, & Son et al., 2021), some studies related to this topic have been briefly presented as follows. Using Finite Element Analysis, Zeng et al. (2019) studied the vibration response characteristics of a fractured spinning compressor blade. Kırıl (2014) investigated the harmonic response of laminated composite beams under a variety of boundary conditions and stacking sequences. The dynamic response of a composite beam

that spins at a constant speed was measured by Gawryluk et al (2019). Abed and Majeed (2020) investigated the influence of boundary conditions on the harmonic response of cross-ply and angle-ply composites of various materials and thicknesses. Both modal and harmonic response studies of carbon fiber laminate reinforced concrete railway sleepers were carried out by Çeçen and Aktaş (2021). Oke and Khulief (2020) conducted a dynamic response study for fluid conveying composite pipes with a surface discontinuity in the inner wall. Zhang et al. (2018) used the dynamic stiffness approach to perform a harmonic analysis for linked plate structures. Yulin et al. (2020) examined the dynamic response of a three-beam system with intermediate elastic connections that was subjected to a moving load while being supported by a mass-spring.

In this study, the effects of cut-out shapes on the fundamental frequency and harmonic response of thin composite circular plates have been measured. For this purpose, the Finite Element Method has been employed by using the SHELL181 element of ANSYS Workbench (Version 18.2). Following the free vibration analysis of circular structures, the harmonic response analysis has been performed by employing the Mode Superposition Method since it solves the harmonic response problem faster than the Full Method without decreasing the accuracy. Although there are numerous studies that comprise the free vibration analysis and harmonic response analysis of various kinds of structures, the impacts of the cut-out shape on the fundamental frequency and harmonic response of thin composite circular plates have not been examined yet. There are many purposes to design a cut-out in structures (e.g., riveting, maintenance, weight reduction, and shifting resonance frequency). Such structures may be subjected to harmonic loadings or vibrations that may cause failure due to excessive vibration. Hence, it is essential to determine the cut-out shape since it may affect the dynamic characteristics of the structure. This study measures the impact of the cut-out shape on the dynamic behavior of thin composite circular plates to provide an understanding of the topic mentioned above. The contribution of the study can be summarized as (i) presenting the effects of the cut-out shape on the fundamental frequency and harmonic response of the thin circular plate, (ii) examining the impact of the fiber orientation on the dynamic properties of thin circular structures having different central cut-outs, and (iii) measuring the relation between the cut-out shape and fiber orientation considering the fundamental frequency and harmonic response of the circular structure.

THE FINITE ELEMENT ANALYSIS OF CIRCULAR STRUCTURES

The Finite Element Analysis has been employed to evaluate the fundamental natural frequency and the harmonic response of composite thin circular plates, shown in Figure 1. The equation of motion of a structure can be written as

$$\mathbf{M}\ddot{\delta} + \mathbf{C}\dot{\delta} + \mathbf{K}\delta = \mathbf{F} \quad (1)$$

where \mathbf{M} , \mathbf{C} , and \mathbf{K} are the mass, damping, and stiffness matrices. δ represents the generalized displacement coordinates vector, and \mathbf{F} is the external force vector. The evaluation of those matrices and vectors can be found in various textbooks (Petyt, 2010). To evaluate the fundamental natural frequency of a structure, it should be considered that there is no external force, and the damping is zero. Therefore, the equation of motion becomes

$$\mathbf{M}\ddot{\delta} + \mathbf{K}\delta = 0 \quad (2)$$

Reducing Equation (2) into an eigenvalue problem gives

$$(\mathbf{K} - \omega_i^2 \mathbf{M})\psi_i = 0 \quad (3)$$

where ω_i is the i^{th} natural frequency of the considered structure, and ψ_i is the corresponding mode shape. To obtain the harmonic response of a structure, the external force and the response should be harmonic. Considering the external force in a complex form as

$$F = F_{max}e^{j\mu}e^{j\Omega t} \tag{4}$$

and the displacement response as

$$r = r_{max}e^{j\gamma}e^{j\Omega t} \tag{5}$$

where Ω is the excitation frequency, γ and μ are the phase shifts of the force and response, respectively. Substituting Equation (5) into Equation (1) and reducing it to eigenvalue problem give

$$(\mathbf{K} + j\Omega\mathbf{C} - \Omega^2\mathbf{M})\psi_i = F \tag{6}$$

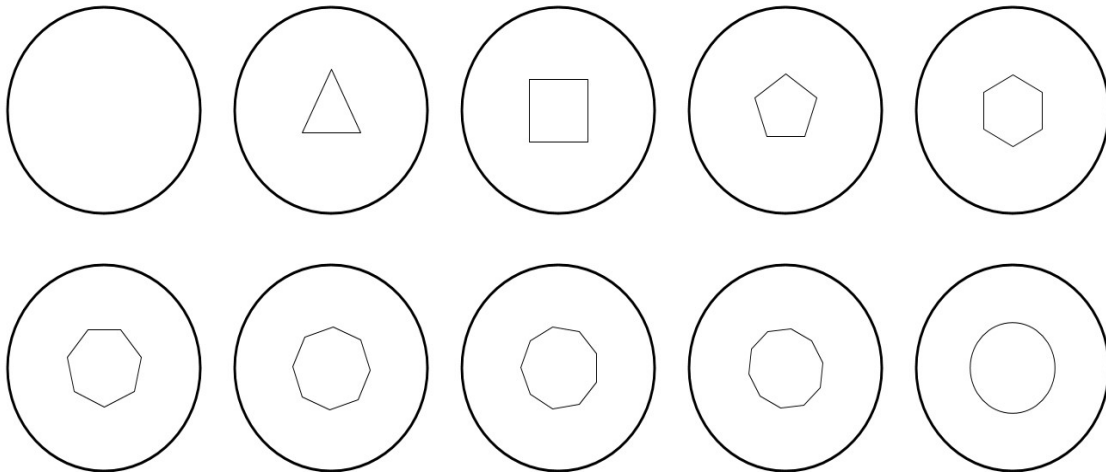


Figure 1. Thin composite circular plates.

Solving Equation (5) using the frequency values that are obtained via Equation (3) gives the response of the structure (Petyt, 2010). In order to perform both free vibration and harmonic response analysis, the SHELL181 element of ANSYS Workbench has been considered. The triangular element having 6 degrees of freedom has been considered for meshing. The adaptive mesh technique has been employed considering the maximum mesh size as 7 mm. All structures have been fixed from their lateral surfaces. To perform the harmonic response analysis, a sinusoidal force with a maximum magnitude of 100 N has been applied on the upper surface of each structure. Figure 2 shows the mesh pattern, applied harmonic force, and the employed boundary condition.

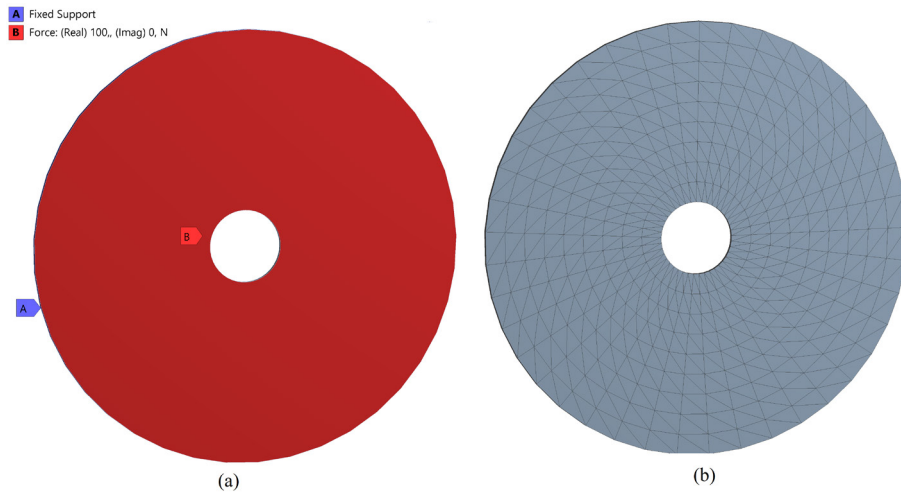


Figure 2. (a) The boundary condition and applied harmonic load; (b) meshed structure.

To solve the harmonic response analysis, the Mode Superposition Method has been considered since it is faster than the Full Method and gives accurate results. The Mode Superposition method requires the eigenvectors or mode shapes, which could be evaluated via the free vibration analysis. Therefore, to investigate the effect of cut-out shape on the fundamental frequency and to satisfy the requirement indicated above, free vibration analysis has been performed on all structures under the same boundary conditions. Afterwards, the frequency range has been determined by multiplying the fundamental frequency by 1.5 to ensure that the response can be observable. To acquire accurate and logical results, the damping effect has been introduced as material damping coefficient by $\xi=0.02$ (Kıral, 2014). As the results show, the diagrams of frequency-displacement, frequency-phase angle, displacement distribution at the critical frequency, and stress distribution at the critical frequency have been interpreted.

NUMERICAL RESULTS

Table 1 presents the geometrical properties of the considered circular structure. As the composite material, unidirectional carbon epoxy composite has been considered. The material has the following properties: $E_x = 121$ GPa, $E_y = E_z = 8.6$ GPa, $G_{xy} = G_{xz} = 4.7$ GPa, $G_{yz} = 3.1$ GPa, $\nu_{xy} = \nu_{xz} = 0.27$, $\nu_{yz} = 0.4$, where E_x , E_y , and E_z are the modulus of elasticity with respect to x -, y -, and z - axis, G_{xy} , G_{xz} , and G_{yz} are the shear modulus with respect to xy -, xz -, and yz - planes, and ν_{xy} , ν_{xz} , and ν_{yz} are the Poisson's ratios in xy -, xz -, and yz - planes, respectively.

Table 1. Geometrical properties of considered structures.

| Property | Symbol | Value |
|--------------------------|--------|------------------------|
| Circular Plate Diameter | d | 300 mm |
| Circular Plate Thickness | t | 3 mm |
| Cut-Out Area | A_c | 1963.5 mm ² |

The effect of the cut-out shape has been investigated by smoothing the shape of the cut-out closer to the circular geometry. The smoothness has been increased by increasing the edge number from 3 to infinite (equilateral triangle to circular). The constant cut-out area has been determined by considering the circular cut-out having a 50 mm diameter. All other cut-outs have been designed considering this constant cut-out area. Therefore, the edge lengths of the cut-outs are different, while their area is the same, which is 1963.5 mm². A comparative analysis has been performed by comparing the results with that of Sun et al. (2021) for validation. For this purpose, a five-layered (0⁰/30⁰/45⁰/60⁰/90⁰) composite circular plates, which have 1000 mm diameter and 10 mm thickness with square cut-outs of 100 x 100 mm, 200 x 200 mm, and 300 x 300 mm, have been considered. The material properties can be found in the corresponding study (Sun et al., 2021). Table 2 shows the comparative analysis results considering nondimensional fundamental frequency, which is evaluated as $\lambda_{nd} = \sqrt{12\lambda_0\rho d^4(1 - \nu_{12}\nu_{21})/E_1t^3}$, where λ is the natural frequency, d is the diameter, E_1 is the modulus of elasticity of the composite material with respect to x-axis, and ν_{12} and ν_{21} are the Poisson’s ratios (Sun et al., 2021).

Table 2. Nondimensional comparative analysis results (Cs: cut-out size).

| Frequency Mode | Cs=100x100 mm | | Cs=200x200 mm | | Cs=300x300 mm | |
|----------------|-----------------------|-------------------|-----------------------|-------------------|-----------------------|-------------------|
| | Present Study (ANSYS) | Sun et al. (2021) | Present Study (ANSYS) | Sun et al. (2021) | Present Study (ANSYS) | Sun et al. (2021) |
| 1 | 13.8769 | 14.0171 | 14.6178 | 14.9673 | 16.8574 | 17.2956 |
| 2 | 27.7943 | 27.7297 | 26.3399 | 26.9835 | 25.5896 | 26.3601 |
| 3 | 28.4032 | 28.3875 | 26.8451 | 27.5683 | 25.9336 | 26.8029 |
| 4 | 44.0324 | 44.3372 | 41.6928 | 42.6750 | 40.7880 | 41.8831 |
| 5 | 45.4892 | 45.1408 | 42.7731 | 43.4541 | 41.3441 | 42.4390 |

It is seen from Table 2 that the free vibration results of the considered method are in close agreement with those of Sun et al. (2021). Tables 3 and 4 give the fundamental frequencies in accordance with cut-out shapes of thin cross-ply and angle-ply circular plates, respectively.

Table 3. Nondimensional fundamental frequencies of cross-ply circular plates.

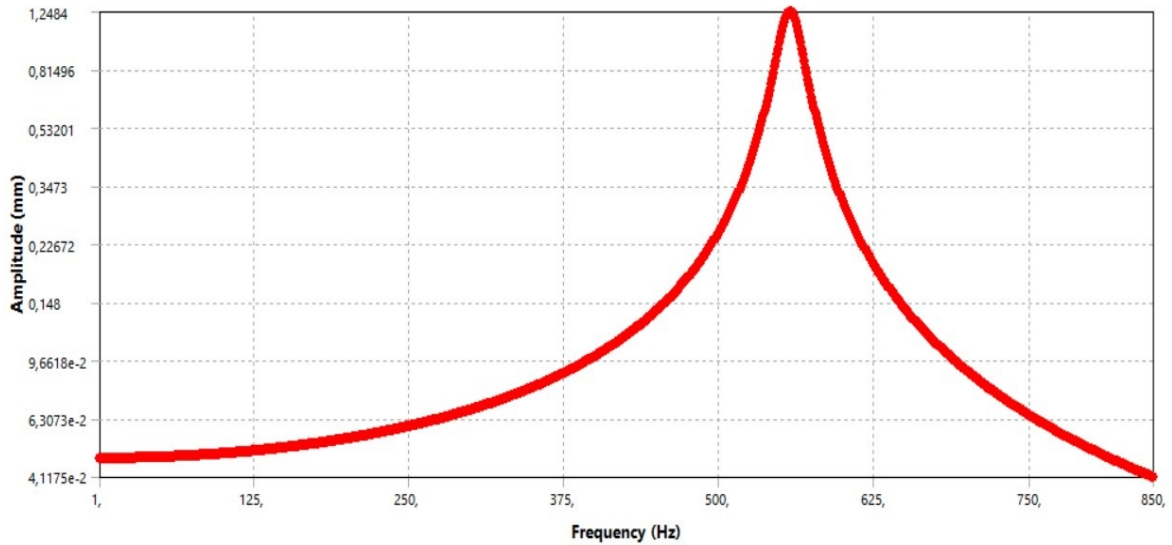
| Frequency (λ_{nd}) | No Cut-Out | Equilateral Triangular Cut-Out | Square Cut-Out | Regular Pentagon Cut-Out | Regular Hexagon Cut-Out |
|---------------------------------|--------------------------------|--------------------------------------|-------------------------------|--------------------------------|-------------------------------|
| 1 | 106.6451 | 136.1910 | 150.6220 | 141.9210 | 150.1756 |
| Frequency (λ_{nd}) | Regular Heptagon Cut-Out | Regular Octagon Cut-Out | Regular Nonagon Cut-Out | Regular Decagon Cut-Out | Circular Cut-Out |
| 1 | 155.9056 | 146.6802 | 144.7556 | 161.6618 | 155.3028 |

Table 4. Nondimensional fundamental frequencies of angle-ply circular.

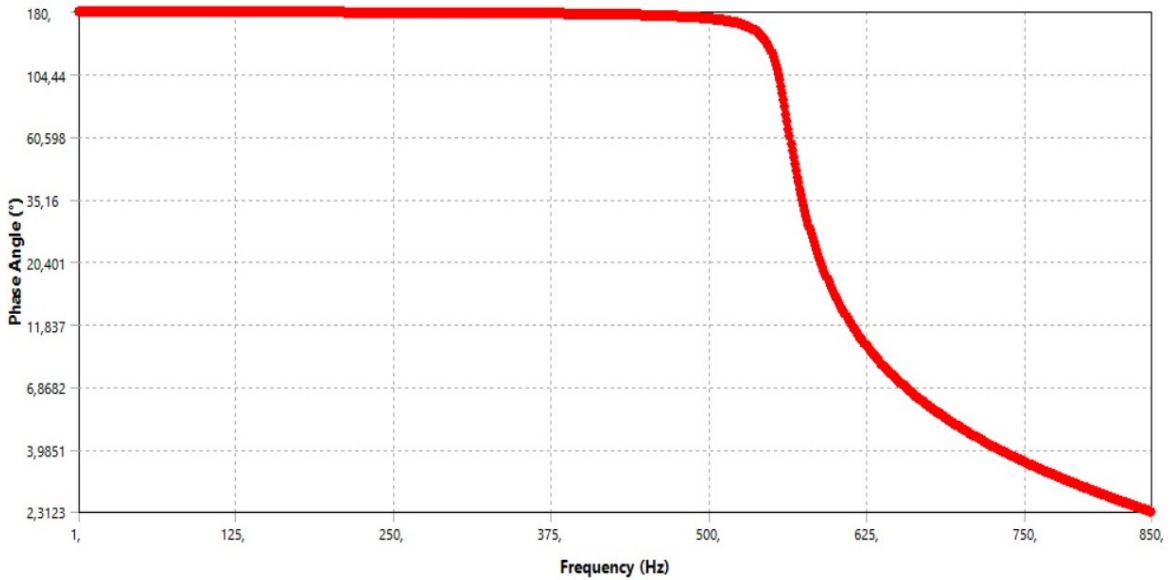
| Frequency (λ_{nd}) | No Cut-Out | Equilateral Triangular Cut-Out | Square Cut-Out | Regular Pentagon Cut-Out | Regular Hexagon Cut-Out |
|---------------------------------|--------------------------------|--------------------------------------|-------------------------------|--------------------------------|-------------------------------|
| 1 | 106.3524 | 135.9156 | 150.6219 | 141.7298 | 150.1234 |
| Frequency (λ_{nd}) | Regular Heptagon Cut-Out | Regular Octagon Cut-Out | Regular Nonagon Cut-Out | Regular Decagon Cut-Out | Circular Cut-Out |
| 1 | 155.6622 | 146.5787 | 144.7093 | 161.4241 | 155.2158 |

According to Tables 4 and 5, the fundamental natural frequencies of the circular plates with cut-outs are higher than those without cut-out. Although the frequency value seems to be an increasing trend, it decreases as the structure has regular pentagon, regular octagon, and regular nonagon cut-outs. Comparing the cut-out, which has the least number of edges (equilateral triangle) and the cut-out that contains an infinite number of edges (circular), it is seen that the fundamental frequency of the circular structure with circular cut out is considerably higher than that of with equilateral triangle cut-out. Considering the fundamental frequencies of the cross-ply and angle-ply structures, it is observed that the fundamental frequencies of the structure with angle-ply fiber orientation are slightly lower (approx. 1Hz) than those of the structure with cross-ply fiber sequence. Tables 5 and 6 show the harmonic response analysis results considering the phase shift, maximum stress, and maximum displacement values. Figure 3 shows the frequency-response and frequency-phase diagram of the cross-ply circular plate having a central regular decagon cut-

out. Note that all other structures have a similar frequency-response and frequency-phase pattern. The only difference is the frequency, response, and phase values. As seen from Figure 3(a), the maximum responses occurred at the fundamental frequency of each structure. The phase shift occurs also at the fundamental frequency for every circular structure.



(a)



(b)

Figure 3. (a) The frequency-displacement response and (b) frequency-phase diagram of cross-ply circular plate having central regular decagon cut-out.

Table 5. Harmonic response analysis results of cross-ply circular plates.

| Parameter | No Cut-Out | Equilateral Triangular Cut-Out | Square Cut-Out | Regular Pentagon Cut-Out | Regular Hexagon Cut-Out |
|----------------------------|---------------------------------|---------------------------------------|--------------------------------|---------------------------------|--------------------------------|
| Phase Shift ($^{\circ}$) | 89.464 | 95.296 | 93.633 | 93.725 | 90.644 |
| Maximum Stress (MPa) | 126.560 | 173.690 | 83.656 | 113.260 | 95.264 |
| Maximum Displacement (mm) | 2.5323 | 1.7661 | 1.4321 | 1.6046 | 1.4527 |
| Parameter | Regular Heptagon Cut-Out | Regular Octagon Cut-Out | Regular Nonagon Cut-Out | Regular Decagon Cut-Out | Circular Cut-Out |
| Phase Shift ($^{\circ}$) | 89.39 | 90.338 | 92.387 | 93.834 | 88.946 |
| Maximum Stress (MPa) | 84.344 | 93.996 | 94.369 | 74.814 | 81.338 |
| Maximum Displacement (mm) | 1.3339 | 1.4988 | 1.5501 | 1.2476 | 1.3455 |

Table 6. Harmonic response analysis results of angle-ply circular plates.

| Parameter | No Cut-Out | Equilateral Triangular Cut-Out | Square Cut-Out | Regular Pentagon Cut-Out | Regular Hexagon Cut-Out |
|----------------------------|---------------------------------|---------------------------------------|--------------------------------|---------------------------------|--------------------------------|
| Phase Shift ($^{\circ}$) | 89.511 | 89.64 | 93.73 | 90.008 | 89.789 |
| Maximum Stress (MPa) | 129.550 | 175.810 | 116.430 | 112.710 | 99.445 |
| Maximum Displacement (mm) | 2.5517 | 1.7805 | 1.4391 | 1.6079 | 1.4481 |
| Parameter | Regular Heptagon Cut-Out | Regular Octagon Cut-Out | Regular Nonagon Cut-Out | Regular Decagon Cut-Out | Circular Cut-Out |
| Phase Shift ($^{\circ}$) | 90.35 | 88.481 | 91.606 | 89.759 | 92.84 |
| Maximum Stress (MPa) | 80.051 | 85.487 | 95.635 | 76.639 | 82.252 |
| Maximum Displacement (mm) | 1.3405 | 1.5032 | 1.5526 | 1.2545 | 1.3541 |

It is seen from Tables 5 and 6 that the maximum phase shift value has been evaluated for the cross-ply circular structure having triangular cut-out (95.296°), while the minimum phase shift has been obtained for the angle-ply circular structure with regular octagon cut-out (88.481°), considering only that the fiber orientation indicates that the phase shift has been slightly affected by fiber angles. The maximum stress value has been obtained for the angle-ply structure with a central equilateral triangular cut-out (175.810 MPa), whereas the minimum stress value has been calculated for the cross-ply structure having a regular decagon cut-out (74.814 MPa). Considering the fiber orientations, it is seen that the only considerable difference in stress values has occurred for the structure with square cut-out, whose stress value is 83.656 MPa for cross-ply orientation and 116.43 MPa for angle-ply sequence. Other structures have also been affected by the change in fiber orientation. However, these changes are small (up to 5MPa) when compared with those that occurred for the square cut-out. Interpreting the displacement values indicate that the maximum displacement has occurred for the angle-ply structure having no cut-out by 2.5517 mm, whereas the minimum displacement has been evaluated for the cross-ply structure with regular decagon cut-out by 1.2476 mm. The fiber orientation has a negligible impact on the displacement of the structure since the maximum displacement difference has been obtained for the structure with no cut-outs by 0.0194 mm. Therefore, it can be concluded that the shape of the cut-out considerably affects the displacement response of the structure. Interpreting all structures in terms of phase values shows that there is no strict increasing or decreasing trend in phase shift values with respect to the edge number of the cut-out or fiber orientation. The stress values fluctuate as the edge number of the cut-out increases. However, in contrast to the phase shifts, the stress values tend to be in a decreasing pattern as the number of edges of the cut-outs increases for all stacking sequences. Similar to the stress trend, the displacement response also shows a decreasing trend in accordance to the increment of the edge number of the cut-outs for both fiber orientations. According to harmonic response analysis results, it has been seen that the distribution of the stress has the same pattern. The stress distributions of cross-ply and angle-ply circular plates have been presented in Figure 4.

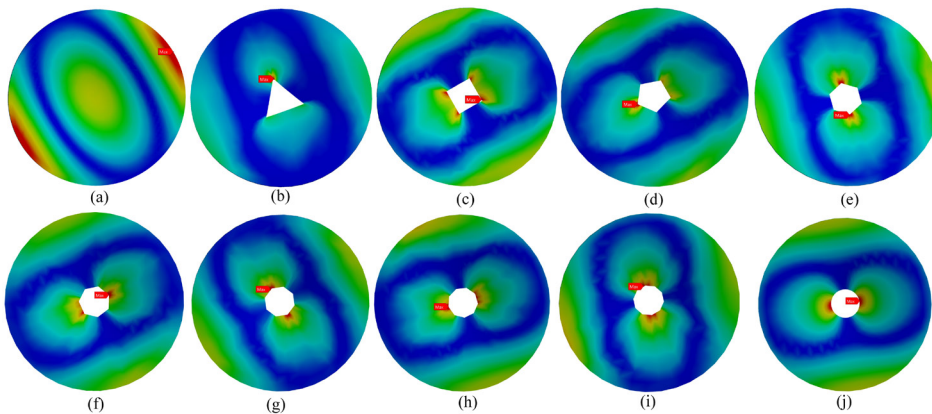


Figure 4. The stress distributions of cross-ply and angle-ply circular structures subjected to harmonic load.

As seen from Figure 4, having any shape of central cut-out moves the maximum stress region to around the cut-out from the edge of the structure. The variation in the shape of cut-outs affects the stress distribution. The blue region represents the lowest stress values (approx. 0 MPa), followed by the light green, green, yellow, and red regions as the regions where the highest stress occurs. It is clearly seen from Figure 4 that the area of light green and green regions becomes smoother as the number of edges of the cut-outs increases. Therefore, the smoothest distribution has been observed for the circular cut-out due to its shape. On the other hand, the stress distribution around the edge and the center of circular structures with cut-outs has also been affected by the cut-out shape. It is seen from Tables 5 and 6 that although the structures with equilateral triangular cut-out have the highest stress values, the stress values change abruptly from the maximum value towards the blue region where the stress is approximately zero. The maximum stress occurrence has been observed at the corners or an edge of the cut-out regardless of its shape. Similar to the

stress values, the displacement values of cross-ply and angle-ply structures are different, whereas the displacement regions are the same. The displacement plots of cross-ply and angle-ply circular plates have been presented in Figure 5.

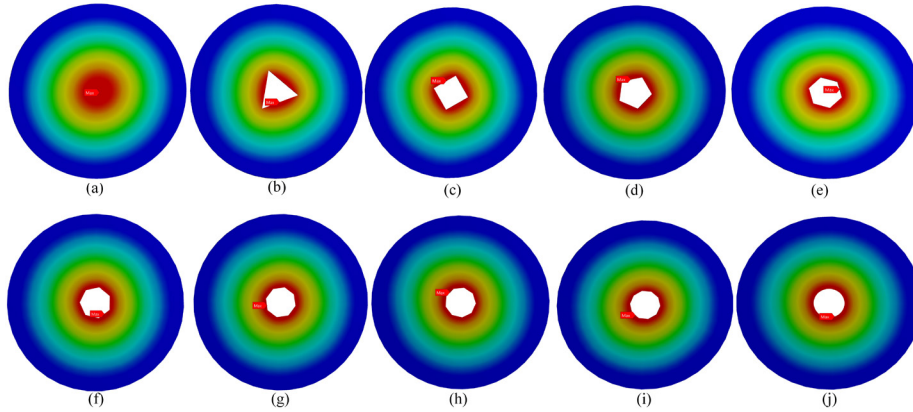


Figure 5. The displacement plots of cross-ply and angle-ply circular structures subjected to harmonic load.

According to displacement plots given in Figure 5, the displacement responses of all structures behave in the same manner regardless of the cut-out existence and the shape of the cut-out. Besides, the displacement plots of all structures are the same as the first mode shapes of all structures.

CONCLUSION

In this study, the impacts of cut-out shape on the fundamental natural frequency and the harmonic response of thin composite circular structures have been measured. According to the numerical results, the following conclusions have been drawn:

- The fundamental frequency values generally increase as the cut-out shape approximates circular geometry no matter which fiber orientation is considered. The phase shift is negligibly affected by the shape of cut-out regardless of the fiber orientation.
- The displacement responses are in decreasing trend as the cut-out shape approximates to circular geometry. The highest displacement is evaluated for the structure with equilateral triangle cut-out, whereas the lowest displacement is obtained for that with regular decagon cut-out.
- The displacement response distribution is the same for all structures regardless of the cut-out existence, cut-out shape, and fiber orientation. The displacement response plots are the same as those of the fundamental mode shape since the maximum response occurred at the fundamental frequency. The fiber orientation does not significantly affect the displacement response.
- The stress values are in decreasing trend as the cut-out shape approximates circular geometry. The highest stress is obtained for the structure with equilateral triangle cut-out, whereas the lowest stress is evaluated for that with the regular decagon cut-out. The fiber orientation slightly affects the maximum stress values, except for the structure with square cut-out.
- The stress distribution has been considerably affected by the cut-out shape. The smoothness of the stress distribution increases as the cut-out shape approximates to circular geometry. The stress regions in which stress values vary from zero to maximum become apparent as the edge number of the cut-out increases.
- The cut-out existence moves the maximum stress from the edge to the center of the structure.

REFERENCES

- Javed, S., Viswanathan, K. K., Nurul Izyan, M. D., Aziz, Z. A., & Lee, J. H. 2018.** Free vibration of cross-ply laminated plates based on higher-order shear deformation theory. *Steel and Composite Structures*. 26 (4): 473-484.
- Gonenli, C., & Das, O. 2021.** Effect of crack location on buckling and dynamic stability in plate frame structures. *Journal of the Brazilian Society of Mechanical Sciences and Engineering*. 43: 311.
- Yui Y., Zhang, S., Li, H., Wang, X., & Tiang, Y. 2017.** Modal and harmonic response analysis of key components of ditch device based on ANSYS. *Procedia Engineering*, 174: 956-964.
- Jiaqiang, E., Liu, G., Liu, T., Zhang, Z., Zuo, H., Hu, W., & Wei, K. 2019.** Harmonic response analysis of a large dish solar thermal power generation system with wind-induced vibration. *Solar Energy*. 181: 116-129.
- Kumar, M., & Sarangi, S. K. 2020.** Harmonic response of carbon nanotube reinforced functionally graded beam by finite element method. *Materials Today: Proceedings*. 44(6): 4531-4536.
- Zeng J., Chen, K., Ma, H., Duan, T., & Wen, B. 2019.** Vibration response analysis of a cracked rotating compressor blade during run-up process. *Mechanical Systems and Signal Processing*. 118: 568-583.
- Kıral, Z. 2014.** Harmonic response analysis of symmetric laminated composite beams with different boundary conditions. *Science and Engineering of Composite Materials*. 21(4): 568-583.
- Gawryluk, J., Mitura, A., & Teter, A. 2019.** Dynamic response of a composite beam rotating at constant speed caused by harmonic excitation with MFC actuator. *Composite Structures*. 210: 657-662.
- Abed, Z. A. K., & Majeed, W. I. 2020.** Effect of boundary conditions on harmonic response of laminated plates. *Composite Materials and Engineering*. 2(2): 125-140.
- Çeçen, F., & Aktaş, B. 2021.** Modal and harmonic response analysis of new CFRP laminate reinforced concrete railway sleepers. *Engineering Failure Analysis*. 127: 105471.
- Oke, W. A., & Khulief, Y. A. 2020.** Dynamic response analysis of composite pipes conveying fluid in the presence of internal wall thinning. *Journal of Engineering Mechanics*. 146(10): 04020118.
- Zhang, C., Jin, G., Ye, T., & Zhang, Y. 2018.** Harmonic response analysis of coupled plate structures using the dynamic stiffness method. *Thin-Walled Structures*. 127: 402-415.
- Yulin, F., Lizhong, J., & Zhou, W. 2020.** Dynamic response of a three-beam system with intermediate elastic connections under a moving load/mass-spring. *Earthquake Engineering and Vibration*. 19(2): 377-395.
- ANSYS® Workbench**, Release 18.2.
- Petyt, M. 2010.** *Introduction to Finite Element Analysis*. Cambridge: Cambridge University Press.
- Sun, X., Zhang, P., Qiao, H., & Lin, K. 2021.** High order free vibration analysis of elastic plates with multiple cutouts. *Archive of Applied Mechanics*. 91: 1837-1858.
- Albassam, B. 2021.** Vibration control of a linear flexible beam structure excited by multiple harmonics. *Journal of Engineering Research*. 9(4B): 410-427.
- Çelebi, K., Yarimpabuç, D., & Baran, T. 2018.** Forced vibration analysis of inhomogeneous rods with non-uniform cross-section. *Journal of Engineering Research*. 6(3): 189-202.
- Sivandi-Pour, A., Farsangi, E. N., Takewaki, I. 2020.** Estimation of Vibration Frequency of Structural Floors Using Combined Artificial Intelligence and Finite Element Simulation. *Journal of Engineering Research*. 8(3): 1-16.